analytical chemistry

Article

Cite This: Anal. Chem. 2018, 90, 4770−4775

pubs.acs.org/ac

Colorimetric Sensor Array for Discrimination of Heavy Metal Ions in Aqueous Solution Based on Three Kinds of Thiols as Receptors

Weiwei He,[†] Long Luo,[‡] Qingyun Liu,[§] and Zhengbo Chen*[,†]

[†]Department of Chemistry, Capital Normal University, Beijing, 100048, China

[‡]Department of Chemistry, Wayne State University, Detroit, Michigan 48202, United States

[§]College of Chemical and Environmental Engineering, Shandong University of Science and Technology, Qingdao, 266590, China

Supporting Information

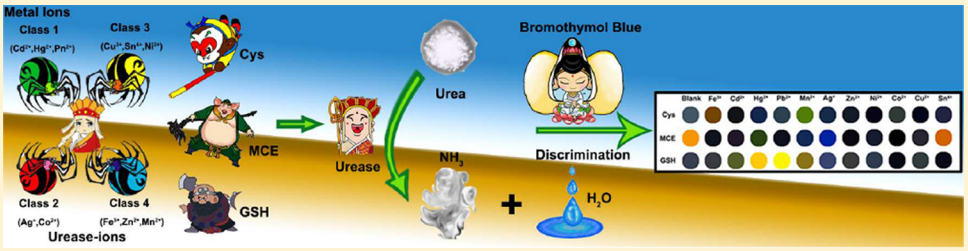

ABSTRACT: In the present work, we report a novel colorimetric sensor array for rapid identification of heavy metal ions. The sensing mechanism is based on the competition between thiols and urease for binding with the metal ions. Due to the different metal ion-binding abilities between the thiols and urea, different percentages of urease are free of metal ions and become catalytically active in the presence of varied metal ions. The metal ion-free urease catalyzes the decomposition of urea releasing ammonia and changing the pH of the analyte solution. Bromothymol blue, the pH indicator, changes its color in response to the metal-caused pH change. Three different thiols (L-glutathione reduced, L-cysteine, and 2-mercaptoethanol) were used in our sensor array, leading to a unique colormetric repsonse pattern for each metal. Linear discriminant analysis (LDA) was employed to analyze the patterns and generate a clustering map for identifying 11 species of metal ions (Ni^{2+}, Mn^{2+}, Zn^{2+}, Ag^{+}, Cd^{2+}, Fe^{3+}, Hg^{2+}, Cu^{2+}, Sn^{4+}, Co^{2+}, and Pb^{2+}) at 10 nM level in real samples. The method realizes the simple, fast (within 30 s), sensitive, and visual discrimination of metal ions, showing the potential applications in environmental monitoring.

Heavy metal ions cause serious human health problems when they enter into the human food chain such as serious damage to the human's central nervous system, liver, kidney, bone, and teeth when they enter into the human food chain.[1−3] Thus, the development of new techniques for a simple, rapid, sensitive, and low-cost identification of toxic metal ions is essential for improving the public health.

Numerous instrumental methods, including atomic absorption spectrometry, spectrophotometry,[4,5] fluorescence,[6,7] and inductively coupled plasma mass spectrometry,[8] have been used for the detection of metal ions. Althought these intrumental methods exhibit high sensitivity and selectivity, their applications are limited by the high-cost and nonportability of these instruments and sophisticated sample preparation, as well as the need of intense technical training. Other heavy metal ion detection methods such as "lock-and-key" sensors require receptors highly specific to the target ions. However, the limited number of available specific receptors hinder the application of these methods. It is thus necessary to develop new receptors as well as the corresponding simple but effective sensing strategies for identification of multiple metal ion targets.

Array-based sensors, which are based on cross-responsive receptors with lower selectivity than specific receptors, simulating the human olfactory or gustatory systems to produce a distinct response pattern of each analyte,[9−15] would be an alternative method to solve this problem. Recently, colorimetric methods for toxic metal ion detection have emerged as a simple and low-cost alternative of spectroscopy-based methods.[16−23] The implementation of colorimetric sensor array strategies not only adopts all the merits of colorimetric methods, but also greatly augments the feasibility of multiple metal ion discrimination.

In this work, we develop a colorimetric sensor array to identify metal ions in aqueous solutions. The sensing mechanism is based on the competitive binding with metal ions between thiols and urease. Different urease-metal ion pairs exhibit diverse affinities toward thiols, generating differential retentions of urease activity and resulting in varying colorimetric responses. The linear discriminant analysis (LDA) and hierarchical cluster analysis (HCA), two unsupervised methods for exploring spectral data without any preliminary information about analytes, were used to analyze these single-channel colorimetric responses and identify

Received: January 6, 2018
Accepted: March 9, 2018
Published: March 9, 2018

DOI: 10.1021/acs.analchem.8b00076
Anal. Chem. 2018, 90, 4770−4775

Scheme 1. Schematic of Three Kinds of Thiols as Receptors-Based Colorimetric Sensor Array for Discrimination of Heavy Metal Ions

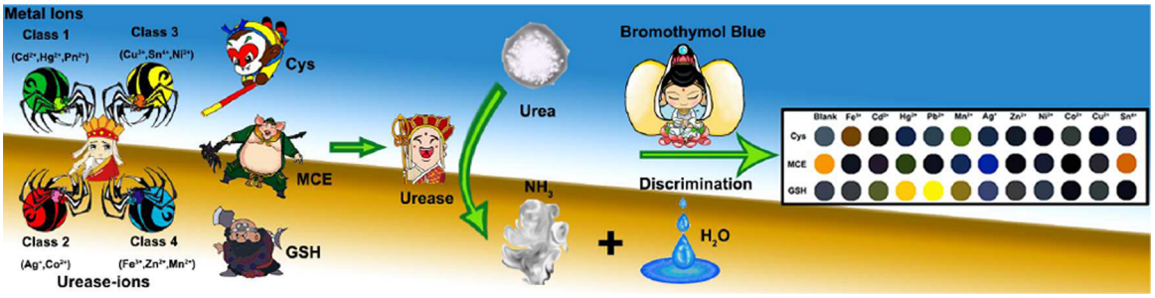

unknown metal ions in the samples. LDA was used to differentiate quantitatively the response patterns of two or more classes of object. HCA, as an alternate method, also was used for identification and differentiation of targets based on Euclidean distance. The two techniques have been commonly utilized for quick discrimination and classification of metal ions.[24−29] Using the sensor array, we have successfully identified 11 different heavy metal ions, including Ni^{2+}, Mn^{2+}, Zn^{2+}, Ag^{+}, Cd^{2+}, Fe^{3+}, Hg^{2+}, Cu^{2+}, Sn^{4+}, Co^{2+}, and Pb^{2+}, with an accuracy of 100%.

EXPERIMENTAL SECTION

Materials. Urease, urea, bromothymol blue, L-glutathione reduced (GSH), L-cysteine (Cys), and 2-mercaptoethanol (MCE) were purchased from Sigma-Aldrich (Shanghai, China). All other reagents are of analytical reagent grade. All solutions were prepared using ultrapure water (18.2 MΩ·cm) from a Milli-Q automatic ultrapure water system.

Instrumentation. Absorption spectra were recorded on SpectraMax^{R}M2e Multi-Mode Microplate Reader (Molecular Devices, California, U.S.A.) at room temperature. The 96-well plates were produced from Costar (3590, U.S.A.).

Experimental Procedure for the Discrimination of Metal Ions. In a 96-well plate, 10 μL of each metal ion (Ni^{2+}, Mn^{2+}, Zn^{2+}, Ag^{+}, Cd^{2+}, Fe^{3+}, Hg^{2+}, Cu^{2+}, Sn^{4+}, Co^{2+}, and Pb^{2+}) with the same concentration was added into 10 μL of urease (0.6 μg/mL) solution and incubated for 10 min at room temperature. Next, 10 μL of each thiol (Cys, GSH, and MCE; 1 μM) was injected into each well, 40 μL of fresh ultrapure water was added, and they were incubated for 15 min at room temperature. Finally, 20 μL of bromothymol blue (0.003%, m/v) and 10 μL of urea (0.1 M) were added to a final volume of 100 μL, and the final concentration of each metal ions is 10 nM. After that, the colorimetric intensity ($A_{594\ nm}$) was recorded. The raw data matrix was processed using classical LDA in SPSS (version 11.03).

RESULTS AND DISCUSSION

Sensing Mechanism. The setup diagram of the thiol-based sensor array for discrimination of heavy metal ions is shown in Scheme 1. Metals ions first bind with urease to form urease−metal ion pairs. In the presence of three kinds of thiols (GSH, Cys, and MCE; Table S1), owing to the high binding affinity between the thiols and the metal ions, these metal ions are taken away from urease−ion pairs by these thiols, and the urease was liberated from urease−metal ion pairs. Thus, the urease is activated to varying degrees and catalyzes the decomposition of urea. The generation of ammonia causes a pH change (6.0−7.6) of the solution, indicated by a color change from yellow to blue with bromothymol blue as the indicator, because the discoloration range of bromothymol blue is just 6.0−7.6. For each metal ion, the sensor array generated a unique colorimetric response pattern that is further differentiated via LDA.

Feasibility Study. According to toxicology of metal elements from strong to weak, we divided metal elements into four levels, that is, Class 1: As, Cd, Hg, and Pb; Class 2: V, Mo, Se, Co, Au, TI, Pd, Pt, Ir, Os, Rh, Ag, and Ru; Class 3: Sb, Ba, Li, Cr, Cu, Sn, and Ni; and Class 4: Al, B, Fe, Zn, K, Ca, Na, Mn, Mg, and W. To test whether our sensor can be used for discrimination of heavy metal ions with different toxicity grades, we investigated the colorimetric responses of the sensor array to four representative metal ions with different toxity grades (Cd^{2+}, Ag^{+}, Sn^{4+}, and Fe^{3+}, each at 10 nM) was investigated (Figure 1). Five replicates were run for each metal ion against three thiols, generating 60 data points (3 thiols × 4 metal ions × 5 replicates). As shown in Figure 1A, the four metal ions exhibited different colormertic patterns with no overlap, which demonstrates the ability of the sensor array to discriminate heavy metal ions. The pattern response data were then analyzed using LDA, which was visualized in a two-dimensional (2D)

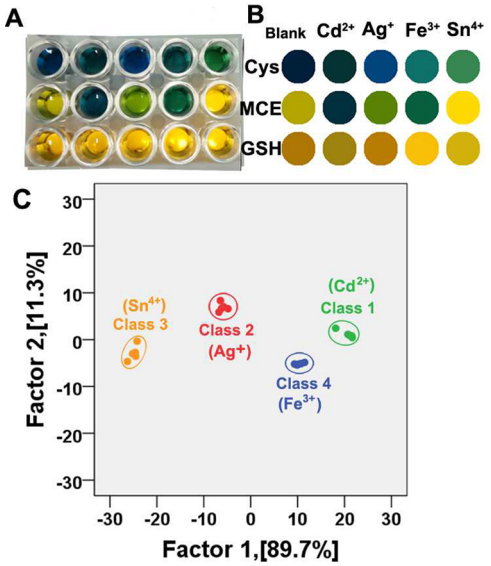

Figure 1. (A) Color patterns of the solutions using three different thiols (Cys, MCE, and GSH) for four classes of metal ions (Class 1: Cd^{2+}, Class 2: Ag^{+}, Class 3: Sn^{4+}, and Class 4: Fe^{3+}) at 10 nM. (B) Digitalized color pattern corresponding to (A). (C) Canonical score plot for the colorimetric response to four metal ions obtained using LDA.

DOI: 10.1021/acs.analchem.8b00076
Anal. Chem. 2018, 90, 4770−4775

plot in Figure 1C under the 95% confidence ellipses. Additionally, the jackknifed classification matrix reveals that the classification accuracy of the 11 metal ions (Ni^{2+}, Mn^{2+}, Zn^{2+}, Ag^{+}, Cd^{2+}, Fe^{3+}, Hg^{2+}, Cu^{2+}, Sn^{4+}, Co^{2+}, and Pb^{2+}) was improved from 76.4% for individual thiol (GSH) to 100% for the combination of Cys, GSH, and MCE (Figure 2 and Table S2). These results demonstrate that our sensing strategy for metal ion discrimination as sensing elements is feasible.

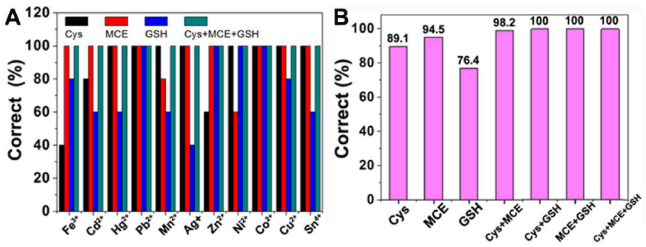

Figure 2. (A) Correct percentage and (B) the classification accuracy for identifying metal ions using an individual thiol (Cys, MCE, or GSH) and the combination of three thiols.

Sensor Optimization. As previously described, the sensor array in this work is based on the recovery of the catalytic activity of urease due to the introduction of thiols, thus, choosing proper concentrations of the three thiols is critical for achieving high sensing performances. Figure 3 shows the absorbance of the sensing solution after the addtion of thiols is strongly dependent on the concentration of thiols. For MCE and GSH, the absorbance decreased with the increasing thiol concentration from 0.1 to 0.25 μM, which may be related to the spatial location of the sulfhydryl of the two thiols. For Cys and GSH, when their concentrations were higher than 1 μM, the absorbance began to decrease. It was possible that the amino and carboxyl groups of the two thiol molecules played important roles in the absorbance change. After taking into considertion the concentration-dependent responses using the three thiols as sensing elements, the optimal concentrations of the three thiols were chosen to 1 μM, where the absorbance values reached the maximum.

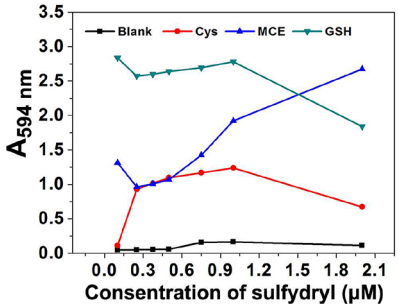

Figure 3. Absorbance of the sensing solution at 594 nm ($A_{594\ nm}$) after adding the thiols with various concentrations (0.1−2.0 μM).

Metal Ion Discrimination. To test the discrimination ability of the colorimetric sensor array, 11 metal ions, including Ni^{2+}, Mn^{2+}, Zn^{2+}, Ag^{+}, Cd^{2+}, Fe^{3+}, Hg^{2+}, Cu^{2+}, Sn^{4+}, Co^{2+}, and Pb^{2+} (each at 10 nM), were chosen as model analytes. The different binding affinities between thiols and metal ions caused differential retentions of urease, leading to unique color shift patterns (Figure 4A,B). Figure 4C and Table S3 illustrate that the array of the three sensor systems each can generate a three-signal fingerprint pattern toward the 11 metal ions. The error bars represent the calculated standard deviation for five replicate measurements. It is apparent that colorimetric signal changes induced by different metal ions were distinct, indicative of the feasibility of metal ion discrimination using the sensor array. The colorimetric signal patterns of the training matrix (3 thiols × 11 metal ions × 5 replicates) were subjected to LDA. As shown in Figure 4D, the contribution of the first two canonical factors was 100% of the total variance (factor 1 = 55.7%; factor 2 = 44.3%). The discriminant analysis results revealed that each metal ion formed tight clusters with a substantial separation between each other. This means that the proposed sensor array could be used to accurately identify metal ions. After successful discrimination of the 11 metal ions at 10 nM, the next step was to determine the limit of detection (LOD) using our sensor array. We prepared the solutions containing 11 metal ions with a concentration of 5 nM and tested them (Figure S1). We found significant overlaps between Fe^{3+}, Co^{2+}, and Ni^{2+} groups and between Mn^{2+}, Cd^{2+}, and Pb^{2+} groups. Thus, the sensor array provides a sensitive discrimination of metal ions with as low as 5 nM. In addition, we

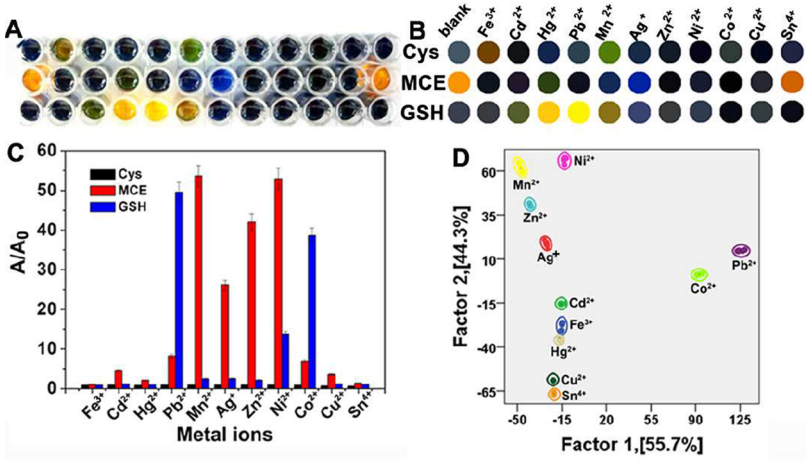

Figure 4. (A) Color change patterns of the solutions using different thiols for different metal ions at 10 nM. (B) Color map corresponding to (A). (C) Fingerprints of the 11 metal ions at 10 nM based on the patterns of the corresponding values of A/A_0 obtained from the colorimetric responses of the sensor array. (D) Canonical score plot for the first two factors of colorimetric signal patterns analyzed by LDA (five parallel measurements).

DOI: 10.1021/acs.analchem.8b00076
Anal. Chem. 2018, 90, 4770−4775

noticed that the same metal ions, but with different conditions, were well separated in the canonical score plot (Figure S2), implying the possible use of the sensor array for quantification of metal ions. Taking Sn^{4+}as an example, the colorimetric responses at various Sn^{4+} concentrations were converted to the total Euclidean distances (EDs = square root of the sums of the square of the normalized (A/A_0) values). Figure 5 shows a EDs

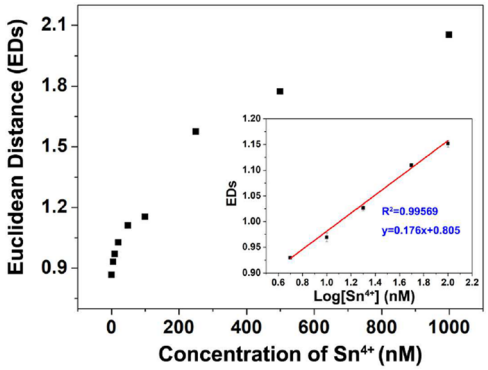

Figure 5. EDs of the sensor array plotted against the different concentrations of Sn^{4+}. Inset: the linear relationship in the logarithm of Sn^{4+} concentration from 5 to 100 nM (error bars illustrate five parallel measurements).

versus dose curve that features a range of 5−1000 nM and a good linearity range from 5 to 100 nM (inset of Figure 5). A LOD of 2.29 nM calculated by the 3σ rule[30] was obtained. In comparison to other sensor arrays for discrimination of metal ions in the literature (Table S4), our sensor array shows the lowest LOD to date. Besides, the discriminatory power of our sensor array is further supported by the HCA result (Figure 6).[31] Remarkably, all 11 metal ion samples were accurately identified, with no error or misclassifications in all 55 cases (11 metal ions × 5 replicates).

With a series of metal ions successfully differentiated, the mixtures of Ag^+ and Cd^{2+} with different molar ratios (Ag^+/Cd^{2+} = 90/10, 70/30, 50/50, 30/70, and 10/90, and the total metal ion concentration was 10 nM) was subsequently tested using the sensor array (Table S5). As shown in Figure 7A, these mixtures, as well as pure Ag^+ and Cd^{2+}, were clearly distinguished from each other in the LDA plot and properly arranged with the order of molar ratios in the dimension of the factor 1. The HCA and LDA results were similar to these mixtures as well, that is, all of the 35 cases were correctly assigned to their respective groups (Figure 7B).

The selectivity of the sensor array was also investigated. As we expected, K^+, Na^+, Mg^{2+}, Al^{3+}, Ca^{2+}, and Fe^{2+}, even at a higher concentration of 100 nM, were introduced to the sensor array as interfering substances. These metal ions could also induce array's responses; however, they were clearly separated from the 11 identified heavy metal ions without any overlap.

To evaluate the robustness of our sensor array, we further measured the colorimetric responses of this sensor array to 55 unknown samples. After adding the thiols to the samples, the absorbance at 594 nm was collected and then analyzed by LDA using the training matrix obtained above (Tables S6−S12). The results show that the 55 unknown samples were correctly identified with an identification accuracy of 100%, indicative of the feasibility of using this sensor array in identifying unknown metal ions.

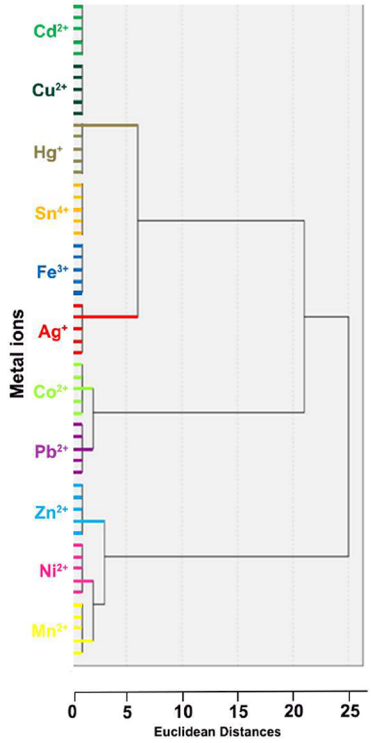

Figure 6. HCA plot for discriminating 11 metal ions (all at 10 nM) based on the colorimetric signal changes of the sensor array.

Discrimination of Metal Ions in Tap Water Samples. To test the applicability of the sensor array, the measurements of the tap water from the Chemical Experimental Building of Capital Normal University. Four kinds of representative metal ions (Cd^{2+}, Ag^+, Sn^{4+}, and Fe^{3+}) in the collected tap water were detected by inductively coupled plasma mass spectrometry (ICP-MS). The tap water samples spiked with the four metal ions, all at 10 nM, have been employed using this sensor array. Each ion corresponds to each toxicity level. Figure 8 and Table S13 show that the tap water itself created a unique array's response, while four metal ion-spiked samples were clustered into four different groups according to the LDA and HCA. The first two canonical factors contained 99.2 and 0.8% of the variation, occupying 100% of the total variation. This finding demonstrates that this sensor array had potentials to discriminate heavy metal ions in real samples. In addition, identification of unknown metal ions in tap water samples also was measured (Tables S14−S17). To further investigate the binding affinity between metal ions and thiols, we performed LDA analysis that incorporates four kinds of metal ions (Cd^{2+}, Ag^+, Sn^{4+}, and Fe^{3+}), corresponding to four toxic levels, each metal ions in a concentration range from 5 to 50 nM (Figure S3). Class 1, as the most serious toxic metal ions, was located in the planes of GSH and MCE. Whereas the least toxic Class 4 is located in the planes of Cys and GSH. Class 2 and Class 3, as medium toxic ions, mainly are concentrated in the planes of GSH and MCE and Cys and GSH, respectively. A small part of Class 2 and Class 3 are located in the planes of MCE and Cys. Thus, we made a conclusion that MCE and Cys play the most important role in identifying Class 1 and Class 4, respectively. For medium toxic Class 2 and Class 3, the binding ability between GSH and them is the strongest.

DOI: 10.1021/acs.analchem.8b00076
Anal. Chem. 2018, 90, 4770−4775

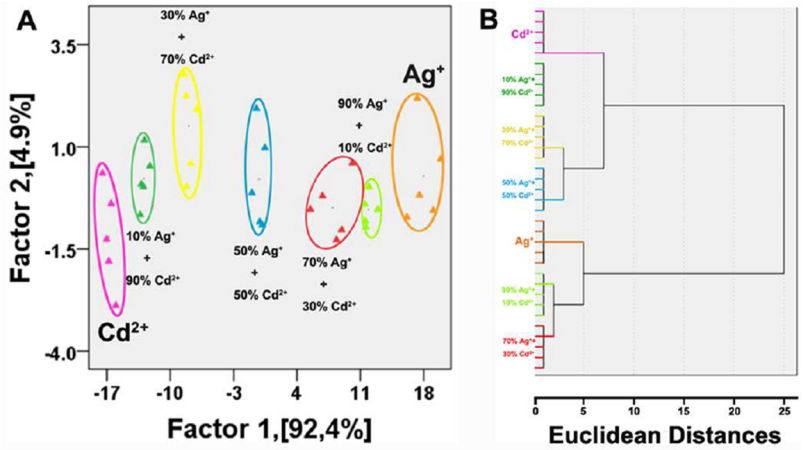

Figure 7. (A) Canonical score plot for the sensor array against metal ion mixtures. Left to right: 100% Cd^{2+}; 10% Ag^+ + 90% Cd^{2+}; 30% Ag^+ + 70% Cd^{2+}; 50% Ag^+ + 50% Cd^{2+}; 70% Ag^+ + 30% Cd^{2+}, 90% Ag^+ + 10% Cd^{2+}, and 100% Ag^+. (B) HCA plot for the sensor array against metal ion mixtures.

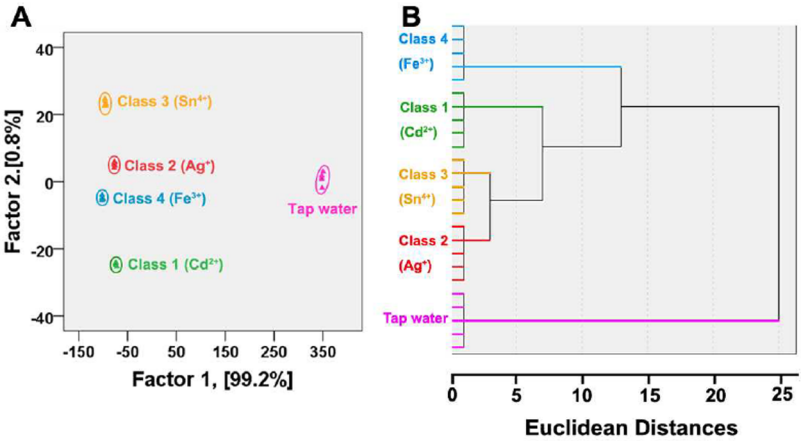

Figure 8. (A) Canonical scores and (B) HCA plots for the discrimination of four tap water samples spiked by different metal ions (all at 10 nM) using the sensor array.

CONCLUSIONS

In summary, we have developed a colorimetric sensor array for the fast and accurate discrimination of heavy metal ions based on three kinds of thiols. The diverse interactions between thiols and metal ions render the dissociation of urease−metal ion pairs to different extent. The released urease catalyzes the conversion of urea to ammonia causing the pH change in the solutions and the consequent color change. Pattern recognition methods (LDA and HCA) were used to evaluate the discrimination performance of the sensor array. The 11 metal ions were successfully identified at a low concentration (10 nM) in aqueous solution with 100% classification accuracy. We further tested tap water spiked with heavy metal ions using our sensor array and achieved 100% correct classification of the metal ions, demonstrating the practical application of our sensor array. The visible sensing paradigm makes the sensor array of important value in rapid on-site environmental monitoring.

ASSOCIATED CONTENT

Supporting Information

The Supporting Information is available free of charge on the ACS Publications website at DOI: 10.1021/acs.analchem.8b00076.

Basic physical properties of thiols. Jackknifed classification matrix obtained using LDA based on Cys, MCE, and GSH. The training matrix of the colorimetric response patterns against 11 metal ions using this sensor assay. Identification of unknown metal ion samples (PDF).

AUTHOR INFORMATION

Corresponding Author

*Tel.: +86-010-68903047. E-mail: czb979216@sina.com.

ORCID

Long Luo: 0000-0001-5771-6892

Zhengbo Chen: 0000-0002-9443-7929

Notes

The authors declare no competing financial interest.

ACKNOWLEDGMENTS

All authors gratefully acknowledge the financial support of Scientific Research Project of Beijing Educational Committee (Grant No. KM201710028009), Youth Innovative Research Team of Capital Normal University, and the Project of Construction of Scientific Research Base by the Beijing Municipal Education Commission.

DOI: 10.1021/acs.analchem.8b00076
Anal. Chem. 2018, 90, 4770−4775

REFERENCES

(1) Aragay, G.; Pons, J.; Merkoci, A. *Chem. Rev.* **2011**, *111*, 3433−3458.
(2) Bush, A. I.; Pettingell, W. H.; Multhaup, G.; Paradis, M. D.; Vonsattel, J. P.; Gusella, J. F.; Beyreuther, K.; Masters, C. L.; Tanzi, R. E. *Science* **1994**, *265*, 1464−1467.
(3) Clarkson, T. W.; Magos, L.; Myers, G. J. *N. Engl. J. Med.* **2003**, *349*, 1731−1737.
(4) Wang, X. D.; Yang, Y. Y.; Dong, J.; Bei, F.; Ai, S. Y. *Sens. Actuators, B* **2014**, *204*, 119−124.
(5) Yan, X.; Li, H.; Yan, Y.; Su, X. *Food Chem.* **2015**, *173*, 179−184.
(6) Hou, J.; Dong, J.; Zhu, H.; Teng, X.; Ai, S.; Mang, M. *Biosens. Bioelectron.* **2015**, *68*, 20−26.
(7) Yan, X.; Li, H. X.; Wang, X. Y.; Su, X. G. *Talanta* **2015**, *131*, 88−94.
(8) Udhayakumari, D.; Suganya, S.; Velmathi, S.; Mubarakali, D. *J. Mol. Recognit.* **2014**, *27*, 151−159.
(9) Albert, K. J.; Lewis, N. S.; Schauer, C. L.; Sotzing, G. A.; Stitzel, S. E.; Vaid, T. P.; Walt, D. R. *Chem. Rev.* **2000**, *100*, 2595−2626.
(10) Zarzo, M. *Biol. Rev.* **2007**, *82*, 455−479.
(11) Wang, J.; Luthey-Schulten, Z. A.; Suslick, K. S. *Proc. Natl. Acad. Sci. U. S. A.* **2003**, *100*, 3035−3039.
(12) You, C. C.; Miranda, O. R.; Gider, B.; Ghosh, P. S.; Kim, I. B.; Erdogan, B.; Krovi, S. A.; Bunz, U. H.; Rotello, V. M. *Nat. Nanotechnol.* **2007**, *2*, 318−323.
(13) Folmer-Andersen, J. F.; Kitamura, M.; Anslyn, E. V. *J. Am. Chem. Soc.* **2006**, *128*, 5652−5653.
(14) Persaud, K.; Dodd, G. *Nature* **1982**, *299*, 352−355.
(15) Askim, J. R.; Mahmoudi, M.; Suslick, K. S. *Chem. Soc. Rev.* **2013**, *42*, 8649−8682.
(16) Sener, G.; Uzun, L.; Denizli, A. *Anal. Chem.* **2014**, *86*, 514−520.
(17) Saha, K.; Agasti, S. S.; Kim, C.; Li, X.; Rotello, V. M. *Chem. Rev.* **2012**, *112*, 2739−2779.
(18) Lou, T.; Chen, Z.; Wang, Y.; Chen, L. *ACS Appl. Mater. Interfaces* **2011**, *3*, 1568−1573.
(19) Zheng, Q.; Han, C.; Li, H. *Chem. Commun.* **2010**, *46*, 7337−7339.
(20) Chai, F.; Wang, C.; Wang, T.; Li, L.; Su, Z. *ACS Appl. Mater. Interfaces* **2010**, *2*, 1466−1470.
(21) Lee, J. S.; Han, M. S.; Mirkin, C. A. *Angew. Chem., Int. Ed.* **2007**, *46*, 4093−4096.
(22) Wu, Y.; Zhan, S.; Wang, F.; He, L.; Zhi, W.; Zhou, P. *Chem. Commun.* **2012**, *48*, 4459−4461.
(23) Dang, Y. Q.; Li, H. W.; Wang, B.; Li, L.; Wu, Y. *ACS Appl. Mater. Interfaces* **2009**, *1*, 1533−1538.
(24) Tan, L. L.; Chen, Z. B.; Zhao, Y.; We, X. C.; Li, Y. H.; Zhang, C.; Wei, X. L.; Hu, X. C. *Biosens. Bioelectron.* **2016**, *85*, 414−421.
(25) Jing, W. J.; Lu, Y. X.; Yang, G. C.; Wang, F. Y.; He, L. Y.; Liu, Y. Y. *Anal. Chim. Acta* **2017**, *985*, 175−182.
(26) Xu, W.; Ren, C. L.; Teoh, C. L.; Peng, J. J.; Haribhau Gadre, S.; Rhee, H. W.; Ken Lee, C. L.; Chang, Y. T. *Anal. Chem.* **2014**, *86*, 8763−8769.
(27) Long, Z.; Fang, D. C.; Ren, H.; Ouyang, J.; He, L. X.; Na, N. *Anal. Chem.* **2016**, *88*, 7660−7666.
(28) Zhou, X. J.; Nie, J. J.; Du, B. Y. *ACS Appl. Mater. Interfaces* **2017**, *9*, 20913−20921.
(29) Wang, S. H.; Ding, L. P.; Fan, J. M.; Wang, Z. X.; Fang, Y. *ACS Appl. Mater. Interfaces* **2014**, *6*, 16156−16165.
(30) Lin, Y. H.; Tseng, W. L. *Chem. Commun.* **2009**, *43*, 6619−6620.
(31) Kong, H.; Lu, Y. X.; Wang, H.; Wen, F.; Zhang, S. C.; Zhang, X. R. *Anal. Chem.* **2012**, *84*, 4258−4261.

DOI: 10.1021/acs.analchem.8b00076
Anal. Chem. 2018, 90, 4770−4775